

In Silico Analysis of Some Phytochemicals as Potent Anti-tubercular Agents Targeting *Mycobacterium tuberculosis* RNA Polymerase and InhA Protein

Md Emran¹, Md Mofijur Rahman¹, Afroza Khanam Anika¹, Sultana Hossain Nasrin¹, Abu Tayab Moin^{2*}

¹Department of Biochemistry and Biotechnology, Faculty of Basic Medical and pharmaceutical Sciences, University of Science and Technology Chittagong, Chattogram, Bangladesh

²Department of Genetic Engineering and Biotechnology, Faculty of Biological Sciences University of Chittagong, Chattogram, Bangladesh

*Correspondence: Abu Tayab Moin, Department of Genetic Engineering and Biotechnology, Faculty of Biological Sciences University of Chittagong, Chattogram, Bangladesh. E-mail: tayabmoin786@gmail.com

Received: November 06, 2020; Accepted: December 08, 2020; Published: December 16, 2020

Copyright: © 2020 Emran Md, et al. This is an open-access article distributed under the terms of the Creative Commons Attribution License, which permits unrestricted use, distribution, and reproduction in any medium, provided the original author and source are credited.

Abstract

Tuberculosis (TB) is a contagious disease, caused by *Mycobacterium tuberculosis* (MTB) that has infected and killed a lot of people in the past. At present treatments against TB are available at a very low cost. Since these chemical drugs have many adverse effects on health, more attention is now given on the plant-derived phytochemicals as potential agents to fight against TB. In this study, 5 phytochemicals, 4-hydroxybenzaldehyde, benzoic acid, bergapten, psoralen, and p-hydroxybenzoic acid, are selected to test their potentiality, safety, and efficacy against two potential targets, the MTB RNA polymerase and enoyl-acyl carrier protein (ACP) reductase, the InhA protein, using various tools of *in silico* biology. The molecular docking experiment, drug-likeness property test, ADME/T-test, P450 SOM prediction, pharmacophore mapping, and modeling, solubility testing, DFT calculations, and PASS prediction study had confirmed that all the molecules had the good potentiality to inhibit the two targets. However, two agents, 4-hydroxybenzaldehyde and bergapten were considered as the best agents among the five selected agents and they also showed far better results than the two currently used drugs, that function in these pathways, rifampicin (MTB RNA polymerase) and isoniazid (InhA protein). These two agents can be used effectively to treat tuberculosis.

Keywords: Tuberculosis; 4-Hydroxybenzaldehyde; Bergapten; Molecular docking.

INTRODUCTION

Tuberculosis (TB) is an ancient disease that plagued mankind many times in the past. It was responsible for many great epidemics. *Mycobacterium tuberculosis* (MTB) is the bacteria that is responsible for tuberculosis disease. These bacteria may have killed more people than any other microbial pathogens [1]. However, at present, tuberculosis is a preventable as well as a curable disease, which is possible at a very low cost. Tuberculosis is a highly contagious disease that can transmit via cough, spit, and sneezes of the infected person. MTB primarily infects the lungs [2-4]. If the disease is found in the lungs, then it is called pulmonary TB. However, TB can be found at other locations of the body. Such TB is called extra-pulmonary TB. Several antibiotics are used to fight against MTB. However, a new TB has emerged in recent years, which is resistant to multiple drugs that are

commonly used in TB treatment. This new TB is called multidrug-resistant tuberculosis (MDR-TB). At present, rifampicin, isoniazid, pyrazinamide, and ethambutol are used all together to treat tuberculosis. However, as the MDR-TB is found to be resistant to multiple drugs that are used in the treatment of normal TB, other sets of drugs are used to treat the MDR-TB [5-7]. Rifampicin inhibits bacterial growth by inhibiting the RNA polymerase enzyme. RNA polymerase enzyme is responsible for synthesizing an RNA strand from a DNA strand by the process known as transcription (Figure 1). Ethambutol exerts its effects by inhibiting the transfer of mycolic acids into the cell wall of MTB as well as by changing the lipid metabolism of the bacteria. Pyrazinamide disrupts the membrane energetics and membrane transport. Thus, pyrazinamide shortens TB therapy [8,9]. Isoniazid, a drug used for treating TB, inhibits bacterial

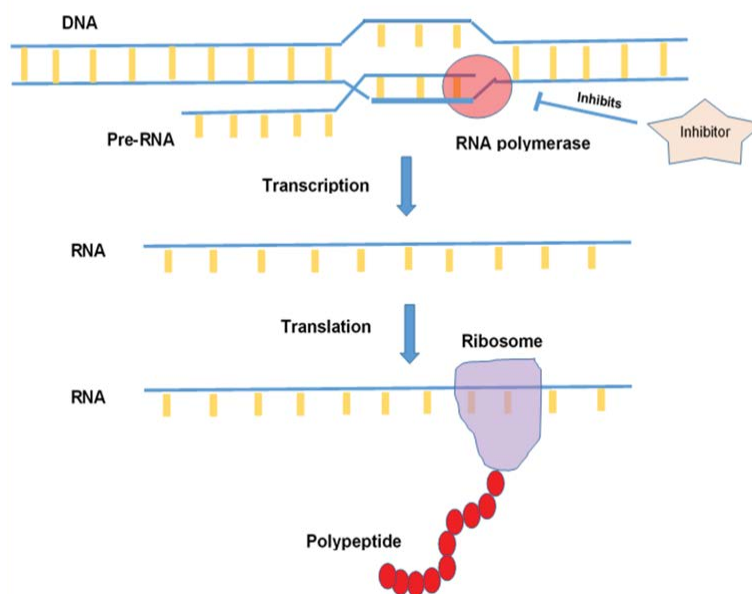
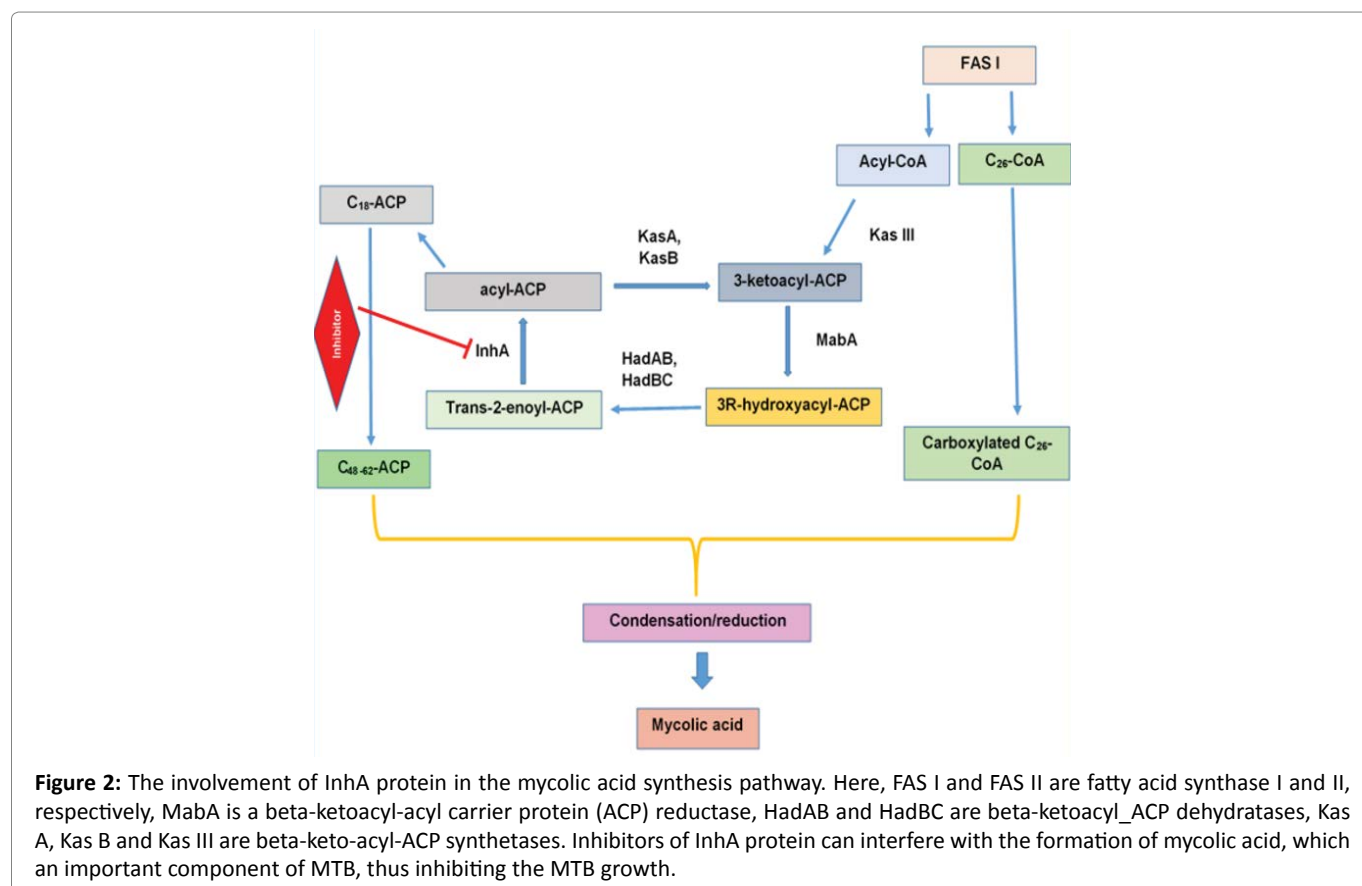


Figure 1: The MTB RNA polymerase functions in the transcription of the MTB DNA. Inhibitors of RNA polymerase can block the function of RNA polymerase, thus aid in inhibiting the bacterial growth.

growth by inhibiting InhA protein, an enoyl-acyl carrier protein (ACP) reductase. The InhA protein is involved in the type II fatty acid biosynthesis pathway as well as mycolic acid synthesis which is an essential component of the bacterial cell membrane [10,11]. In the mycolic acid synthesis pathway, two types of fatty acid synthase (FAS) enzymes are involved: FAS I and FAS II. The FAS I enzyme generates the starting material of the mycolic acid synthesis, acetyl-CoA. The acyl-CoA is converted to 3-ketoacyl-ACP by Kas III enzyme (beta-ketoacyl-ACP synthase III). The 3-ketoacyl-ACP then enters into a cyclic reaction catalyzed by the FAS II enzyme. 3-ketoacyl-ACP is converted into 3R-hydroxyacyl-ACP by beta-ketoacyl-ACP reductase enzyme, MabA. The 3R-hydroxyacyl-ACP is later converted to trans-2-enol-ACP by beta-hydroxyacyl-ACP dehydratases, HadAB and HadBC. Next, the trans-2-enol-ACP is converted to acetyl-ACP by the InhA protein. The acyl-ACP can be converted to either 3-ketoacyl-ACP to start the cycle again (catalyzed by beta-keto-acyl-ACP synthetases, KasA and KasB proteins), or it can be converted to higher chained ACP like C18-ACP and later the C18-ACP forms ever higher chained ACP like C48-ACP to C62-ACP. Moreover, FAS I also generate carboxylated C26-CoA, which together with C48-C62-ACP, undergoes condensation/reduction reaction and forms mycolic acid (Figure 2). The inhibitors of InhA enzyme acts by inhibiting InhA and thus prevents the mycolic acid synthesis [12-14].

Computational methods are now extensively used in drug R&D processes. Such virtual screening methods reduce both time and cost of the drug discovery and development processes. Computational simulation tools are used in designing more than 50 drugs to this date and many of them have received FDA approval. Molecular docking predicts the interaction, pose, and conformation of a ligand within the binding site of a target molecule. After estimating the interactions, the software assigns scores to each of the bound ligands with a specified algorithm which reflects the binding affinity. Lowest score of binding (lowest docking score) represents the most appreciable interaction between the ligand and receptor [15,16].

Natural agents from plants like 4-hydroxybenzaldehyde, benzoic acid, bergapten, Psoralen, p-hydroxybenzoic acid and many other compounds are proved to exhibit anti-tuberculosis properties in various studies [17-19]. The agents can be extracted from a variety of plant sources (Table 1). In this experiment, the two commercially available and mostly used drugs, rifampicin against MTB RNA polymerase and isoniazid against the InhA protein, were used as controls. The mentioned five ligands: 4-hydroxybenzaldehyde, benzoic acid, bergapten, psoralen and p-hydroxybenzoic acid, are used to dock against the MTB RNA polymerase and the InhA protein to test their efficacy and potentiality against the enzymes. Later, the two best ligands, each against one enzyme, were determined



by analyzing the various tests that are conducted in the experiment and the two ligands were compared with the control to test their efficiency to inhibit TB.

No.	Name of the anti-tuberculosis agent	Plant source
1	4-hydroxybenzaldehyde	<i>Cinnamomum kotoense</i>
2	Benzoic acid	<i>Hibiscus taiwanensis</i>
3	Bergapten	<i>Fatoua pilosa</i>
4	Psoralen	<i>Fatoua pilosa</i>
5	p-hydroxybenzoic acid	<i>Microtropis fokiensis</i>

Table 1: Table showing anti-tuberculosis agents with their respective plant sources.

MATERIALS AND METHODS

By applying Maestro-Schrödinger Suite 2018-4, Ligand preparation, Grid generation, Glide docking, and 2D representations of the best pose interactions between the ligands and their particular receptors were achieved. Using Discovery Studio Visualizer [20,21], the 3D representations of the superior pose interactions between the ligands and their receptors were visualized. 2D structures of the ligands were downloaded in SDF format from PubChem (<https://pubchem.ncbi.nlm.nih.gov>). Besides, from the protein data bank (www.rcsb.org), the two receptors were downloaded.

Preparation of Protein

From protein data bank (www.rcsb.org), the 3D structure of InhA protein (PDB ID: 2NSD) and MTB RNA polymerase (PDB ID: 6M7J) were downloaded in PDB format. Preparation and refinement of these proteins were carried out using the Protein Preparation Wizard in Maestro Schrödinger Suite 2018-4 [22]. Assignment of bond orders and the addition of hydrogens to heavy atoms were conducted. The conversion of Selenomethionines to methionines as well as deletion of water was performed. The structure was finally optimized and, next, minimized applying force field OPLS_2005.

Ligand Preparation and Receptor Grid Generation

The 2D conformations of 4-hydroxybenzaldehyde (PubChem CID: 126), Benzoic acid (PubChem CID: 243), Bergapten (PubChem CID: 2355), Psoralen (PubChem CID: 6199), and p-hydroxybenzoic acid (PubChem CID: 135) were downloaded from PubChem (www.pubchem.ncbi.nlm.nih.gov), maintaining sequestration. With the help of the Galaxy 3D Structure Generator v2018.01-beta tool of online server Molinspiration chemoinformatics (<https://www.molinspiration.com/>), the visualization of 3D conformers of the ligands was done. Afterward, these

structures were prepared using the LigPrep function of Maestro Schrödinger Suite 2018-4 [23].

Generally, the grid confines the active site to shortened particular receptor protein areas for the ligand to dock precisely. A grid was produced in Glide utilizing default Van der Waals radius scaling factor 1.0 and charge cutoff 0.25 that was subsequently exposed to the OPLS_2005 force field. A cubic box was created surrounding the active site (reference ligand active site). After that, for conducting a docking test, the grid box volume was customized to 15×15×15.

Glide Standard Precision (SP) Ligand Docking and MM-GBSA Prediction

SP adaptable glide docking was performed by applying Glide in Maestro Schrödinger Suite 2018-4. The Van der Waals radius scaling factor and charge cutoff was adjusted to 0.80 and 0.15 accordingly for each ligand molecule. Using Maestro Schrödinger Suite 2018-4, the 2D and 3D pose interactions between the ligands and receptors were visualized. Moreover, the ligand molecule's interaction with different amino acids and their bonds was analyzed using Discovery Studio Visualizer. The molecular mechanics- generalized born and surface area (MM-GBSA) tool was applied for determining the ΔG_{Bind} scores. The MM-GBSA study was conducted by Maestro-Schrödinger Suite 2018-4.

Ligand Based Drug Likeness Property and ADME/ Toxicity Prediction

The analysis of each ligand's molecular structure was conducted using the SWISSADME server (<http://www.swissadme.ch/>) to ensure whether they abide by Lipinski's rule of five or not, accompanying a few other properties. Calculation of Different physicochemical properties of ligand molecules were performed using OSIRIS Property Explorer (<https://www.organic-chemistry.org/prog/peo/>). The drug-likeness properties of the chosen ligand molecules were analyzed by the SWISSADME server (<http://www.swissadme.ch/>) and the OSIRIS Property Explorer (<https://www.organic-chemistry.org/prog/peo/>) (Organic Chemistry Portal. <https://www.organic-chemistry.org/prog/peo/>. 10/10/2019. Accessed: 09 August 2019). Using online based servers i.e., admetSAR (<http://lmmd.ecust.edu.cn/admetSar2/>) and ADMETlab (<http://admet.scbdd.com/>), the ADME/T for every ligand molecule was conducted for predicting their several pharmacodynamic and pharmacokinetic properties. Both admetSAR and ADMETlab servers are widespread tools for determining

the absorption, distribution, metabolism, excretion, and toxicity of different chemical compounds [24,25].

P450 Site of Metabolism (SOM) Prediction

The P450 Site of Metabolism (SOM) of the selected ligand molecules was checked by an online tool, RS-WebPredictor 1.0 (<http://reccr.chem.rpi.edu/Software/RS-WebPredictor/>) [26]. The probable sites of metabolism on selected ligands were determined for the CYP 450 enzyme family's nine isoforms: CYPs 1A2, 2A6, 2B6, 2C19, 2C8, 2C9, 2D6, 2E1, and 3A4.

Pharmacophore Modelling

The five ligands' pharmacophore modelling was performed by the Phase pharmacophore perception engine of Maestro-Schrödinger Suite 2018-4. The pharmacophore modelling was hand-operated. The radii sizes were maintained as the van der Waals radii of receptor atoms to conduct this process. The radii scaling factor was set to 0.50, receptor atoms whose surfaces are inside 2.00 Å of the ligand surface were neglected, and the volume shell thickness was restricted to 5.00 Å. The 2D and 3D pharmacophore modelling were performed for each ligand molecule.

Prediction of Solubility

The solubility testing of the five ligands was performed using the QikProp wizard of Maestro-Schrödinger Suite 2018-4. In solubility prediction, the selected ligands' solubility was determined in various interfaces like hexadecane/gas interface, octanol/gas interface, octanol/water interface, etc.

DFT Calculation

Minimized ligand structures attained from LigPrep were used for DFT calculation by the application of Jaguar panel of Maestro Schrödinger Suite v11.4, where Becke's three-parameter exchange potential and Lee-Yang-Parr correlation functional (B3LYP) theory with 6-31G* basis set was used [27,28]. Quantum chemical properties, particularly surface properties (MO, density, potential) as well as Multipole moments were determined accompanied by HOMO (Highest Occupied Molecular Orbital) and LUMO (Lowest Unoccupied Molecular Orbital) energy. Afterward, the analysis of global frontier orbital was performed; also, the calculation of hardness (η) and softness (S) of selected molecules was done using the following equation according to Koopmans theorem and Parr and Pearson interpretation [29,30].

$$\eta = (\text{HOMO}\epsilon - \text{LUMO}\epsilon)/2,$$

$$S = 1/\eta$$

2.09. PASS (Prediction of Activity Spectra for Substances) Prediction Study

The PASS (Prediction of Activity Spectra for Substances) prediction was performed only for the two best-selected ligands that displayed the best result in inhibiting their individual receptors, MTB RNA polymerase as well as InhA protein. PASS prediction was conducted by using the PASS-Way2Drug server (<http://www.pharmaexpert.ru/passonline/>), which is operated by canonical SMILES from PubChem server (<https://pubchem.ncbi.nlm.nih.gov/>) [31]. For conducting PASS prediction, Pa (probability "to be active") was held to more than 70% because the Pa > 70% threshold gives highly reliable prediction [32]. In the PASS prediction study, the probable biological activities and the probable adverse consequences of the selected ligands were predicted. The LD50 and Toxicity class prediction was completed using the ProTox-II server (http://tox.charite.de/protox_II/) [33].

RESULTS

Molecular Docking Study and Ramachandran Plot Analysis

All the selected ligand molecules and the controls were docked successfully with their target receptors, MTB RNA polymerase and MTB InhA protein. The controls, rifampicin and isoniazid generated docking scores of -4.813 Kcal/mol (with MTB RNA polymerase) and -6.018 Kcal/mol (with the InhA protein), respectively. 4-hydroxybenzaldehyde yielded docking scores of -6.062 Kcal/mol with RNA polymerase and -7.161 Kcal/mol with InhA protein. Benzoic acid showed docking scores of -5.383 Kcal/mol with RNA polymerase and -7.302 Kcal/mol with InhA protein. Bergapten came up with the docking scores of -5.290 Kcal/mol when docked against RNA polymerase and -8.068 Kcal/mol with InhA protein. Psoralen generated docking scores of -5.731 Kcal/mol with RNA polymerase and -7.102 Kcal/mol when docked against InhA protein. Moreover, p-hydroxybenzoic acid generated docking scores of -4.617 Kcal/mol with RNA polymerase and -7.538 Kcal/mol with InhA protein. From the docking study, it is clear that 4-hydroxybenzaldehyde generated the lowest score of -6.062 Kcal/mol with RNA polymerase and bergapten generated the lowest score of -8.068 Kcal/mol with InhA protein.

On the other hand, all the ligands and the controls also gave successful results in the MM-GBSA study. In the MM-GBSA study, the Δ GBind score was determined. Rifampicin and isoniazid generated Δ GBind scores of

-34.317 Kcal/mol and -29.728 Kcal/mol, respectively. 4-hydroxybenzaldehyde generated Δ GBind scores of -53.070 Kcal/mol with RNA polymerase and -34.240 Kcal/mol with InhA protein. Benzoic acid showed Δ GBind scores of -40.810 Kcal/mol with RNA polymerase and -40.440 Kcal/mol with InhA protein. Bergapten generated Δ GBind scores of -42.390 Kcal/mol and -57.590 Kcal/mol with InhA protein. Psoralen generated Δ GBind scores of -43.150 Kcal/mol with RNA polymerase and -55.330 Kcal/mol with InhA protein. Furthermore, p-hydroxybenzoic acid generated Δ GBind scores of -37.53 Kcal/mol with RNA polymerase and -45.740 Kcal/mol with InhA protein. The MM-GBSA study confirmed that 4-hydroxybenzaldehyde also generated the lowest Δ GBind score of -53.070 Kcal/mol like the docking study with RNA polymerase as well as bergapten generated the lowest Δ GBind score of -57.590 Kcal/mol with InhA protein.

Bergapten formed the highest number of hydrogen bonds with both RNA polymerase (05) as well as InhA protein (08). Bergapten also interacted with the highest number of amino acids within the binding pocket of RNA polymerase. It interacted with 05 amino acids: Arg 421, Val 422, Leu 1089, Ile 1253 and Gly 1069 when docked against MTB RNA polymerase. On the other hand, it also interacted with 07 amino acids within the binding pocket of InhA protein: Lys 165, Gly 96, Ile 194, Gly 192, Ala 191, Ile 21 and Met 147. 4-hydroxybenzaldehyde also interacted with 07 amino acids when docked against InhA protein: Met 147, Lys 165, Ile 194, Ile 21, Pro 193, Gly 192 and Ala 191. The docking scores, glide energy and glide ligand efficiency of the controls are listed in Table 2. The docking scores, glide energies, glide ligand efficiency scores, Δ GBind scores, number of hydrogen bonds, interacting amino acids as well as different types of bonds and their distances are listed in Table 3. Figures 3-5 illustrate the 2D and 3D representations of the best interaction between the ligands and receptors as well as the various amino acids that take part in the interaction.

Druglikeness Properties

All the ligands obeyed the Lipinski's rule of five: molecular weight (acceptable range: ≤ 500), the total number of hydrogen bond donors (acceptable range: ≤ 5), total number of hydrogen bond acceptors (acceptable range: ≤ 10), lipophilicity (LogP, acceptable range: ≤ 5) and molar refractivity (40-130) [34]. Bergapten had the highest molecular weight of 216.19 g/mol. 4-hydroxybenzaldehyde and benzoic acid showed a similar molecular weight of 122.12 g/mol, which was

Table 2: Results of molecular docking between the controls and their receptors.

Name of the control	Name of the receptors	Docking score/ binding energy (Kcal/ mol)	Glide energy (Kcal/mol)	Glide ligand efficiency (Kcal/ mol)	MM-GBSA (Δ GBind Score Kcal/mol)
Rifampicin (PubChem CID: 135398735) (Control-1)	MTB RNA Polymerase (PDB ID: 6M7J)	-4.813	-25.247	-0.503	-34.317
Isoniazid (PubChem CID: 3767) (Control-2)	InhA protein (2NSD)	-6.018	-29.728	-0.602	-25.12

Table 3: Results of molecular docking between ligands and receptors. All the selected ligands were docked successfully against the MTB RNA polymerase and InhA protein.

Name of receptor	Name of ligand	Docking score/ binding energy (Kcal/mol)	Glide energy (Kcal/mol)	Glide ligand efficiency (Kcal/mol)	MM- GBSA (Δ GBind Score Kcal/mol)	No of hydrogen bonds with amino acids	Interacti ng amino acids	Bond distance in A	Types of bonds
MTB RNA Polymerase (PDBID: 6M7J)	4- hydroxybenz aldehyde (PubChemCID: 126)	-6.062	-21.269	-0.674	-53.07	4	Gln 882	2.56	Conventional
							Lys 1249	4.5	Pi-Alkyl
							Asp 879	3.35	Pi-Cation
							Trp 1074	1.65	Conventional
	Benzoic acid (PubChemCID: 243)	-5.383	-21.786	-0.598	-40.81	2	Gly 408	4.92	Pi-Pi stacked
							Ala 1224	3.58	Pi-Pi stacked
							Leu1221	2.72	Conventional
							Ile 1253	2.15	Conventional
	Bergapten (PubChemCID: 2355)	-5.29	-30.331	-0.331	-42.39	5	Arg 421	4.28	Pi-Alkyl
							Val 422	5.28	Pi-Alkyl
							Leu 1089	5.39	Pi-Alkyl
							Gly 1069	2.19	Conventional
Psoralen (PubChem CID: 6199)	p- hydroxybenz oic acid (PubChem CID: 135)	-4.617	-24.02	-0.462	-37.53	3	Ile 1253	2.78	Conventional
							Leu 1089	5.02	Pi-Alkyl
							Lys 420	4.93	Pi-Alkyl
							Gly 419	5.35	Pi-Alkyl
							Ile 1253	2.55	Carbon
							Gly 1069	2.55	Carbon
	Leu 1089	-5.731	-26.147	-0.409	-43.15	4	Leu 1089	4.23	Pi-Alkyl
							Cys 1073	4.26	Pi-Alkyl
							Gln 1069	5.38	Pi-Alkyl
							Lys 420	5.33	Pi-Alkyl
InhA protein (2NSD)	4-hydroxybenz aldehyde (PubChem CID: 126)	-7.161	-26.863	-0.796	-34.24	4	Lys 420	2.66	Carbon
							Gly 419	2.06	Conventional
							Ile 1253	2.71	Carbon
							Leu 1089	2.84	Conventional
							Lys 420	2.14	Conventional
							Gly 419	2.9	Pi-Sigma
4-hydroxybenz aldehyde (PubChem CID: 126)	-7.161	-26.863	-0.796	-34.24	-34.24	4	Lys 165	5.26	Pi-Alkyl
							Met 147	2.47	Pi-Donor
							Ile 21	2.69	Carbon
							Ile 194	2.43	Conventional
							Pro 193	2.07	Conventional
							Gly 192	5.41	Pi-Alkyl
4-hydroxybenz aldehyde (PubChem CID: 126)	-7.161	-26.863	-0.796	-34.24	-34.24	4	Ala 191	5.41	Pi-Alkyl
							Ala 191	5.41	Pi-Alkyl

InhA protein (2NSD)	Benzoic acid (PubChem CID: 243)	-7.302	-29.106	-0.811	-40.44	3	Ile 21	5.35	Pi-Alkyl
							Ala 191	4.79	Pi-Alkyl
							Pro 193	2	Conventional
								2.7	Carbon
	Bergapten (PubChem CID: 2355)	-8.068	-35.218	-0.304	-57.59	8	Ile 194	2.18	Conventional
							Lys 165	2.14	Conventional
							Gly 96	2.95	Carbon
								3.09	Carbon
							Ile 194	2.81	Carbon
								Gly 192	2.25
							Ala 191	2.87	Carbon
								4.4	Pi-Alkyl
	Ile 21	5.08	Pi-Alkyl						
		Met 147	5.3	Pi-Alkyl					
	5.4		Pi-Alkyl						
	Psoralen (PubChem CID: 6199)	-7.102	-32.59	-0.507	-55.33	2	Pro 193	2.88	Carbon
							Ile 194	1.96	Conventional
								5.36	Pi-Alkyl
							Ile 21	5.21	Pi-Alkyl
								Ala 191	5.17
Met 147							5.22	Pi-Alkyl	
	5.25	Pi-Alkyl							
p- hydroxybenz oic acid (PubChem CID: 135)	-7.538	-32.452	-0.754	-45.74	4	Ile 21	5.39	Pi-Alkyl	
						Ala 191	5	Pi-Alkyl	
						Asp 148	1.85	Conventional	
						Ile 194	1.79	Conventional	
							1.89	Conventional	
Pro 193	2.55	Carbon							

the lowest among all the ligands. The highest consensus Log Po/w value was shown by bergapten (2.16), and the lowest value was generated by p-hydroxybenzoic acid of 1.05. However, bergapten showed the lowest LogS value of -2.93, and 4-hydroxybenzaldehyde showed the LogS value of -1.87. Both 4-hydroxybenzaldehyde and benzoic acid had two hydrogen bond acceptors each and one hydrogen bond donors each. Bergapten had four hydrogen bond acceptors, and psoralen had three hydrogen bond acceptors; however, both of them did not have any hydrogen bond donors. P-hydroxybenzoic acid had three hydrogen bond acceptors and two hydrogen bond donors. P-hydroxybenzoic acid possessed the largest topological polar surface area (TPSA) of 57.53 Å². However, both 4-hydroxybenzaldehyde and benzoic acid showed similar TPSA value of 37.30 Å², which was the lowest TPSA value. Benzoic acid had the highest drug-likeness score of -1.4, and 4-hydroxybenzaldehyde had the lowest score of -6.31. P-hydroxybenzoic acid generated the highest drug score of 0.35, and bergapten generated the lowest drug score of 0.10. However, only bergapten was found to be reproductive effective and tumorigenic. Furthermore, only 4-hydroxybenzaldehyde and benzoic acid were irritant, and all the ligands were

found to be mutagenic. The values of the drug-likeness properties are listed in Table 4.

ADME/T Test

The results of the ADME/T test are listed in Table 5. In the absorption section, all the selected ligands showed Caco-2 permeability and human intestinal absorption capability. However, all of them were not p-gp inhibitor as well as p-gp substrate. In the distribution section, all of the ligands showed blood-brain barrier permeability. However, p-hydroxybenzoic acid and 4-hydroxybenzaldehyde showed relatively low plasma protein binding capability than the other three ligands. In the metabolism section, 4-hydroxybenzaldehyde, benzoic acid and p-hydroxybenzoic acid were non-inhibitors as well as non-substrate for all the CYP450 isoenzymes. However, due to the unavailability of data in the server, the CYP450 1A2 and CYP450 2C19 substrates were not determined. However, bergapten and psoralen showed quite similar results in the metabolism section with inhibitory effects on the CYP450 1A2, 3A4, 2C9, 2D6 and 2C19. In the excretion section, 4-hydroxybenzaldehyde had the highest half-life of 1.7 h. In the toxicity section, none of the molecules was hERG blocker and only

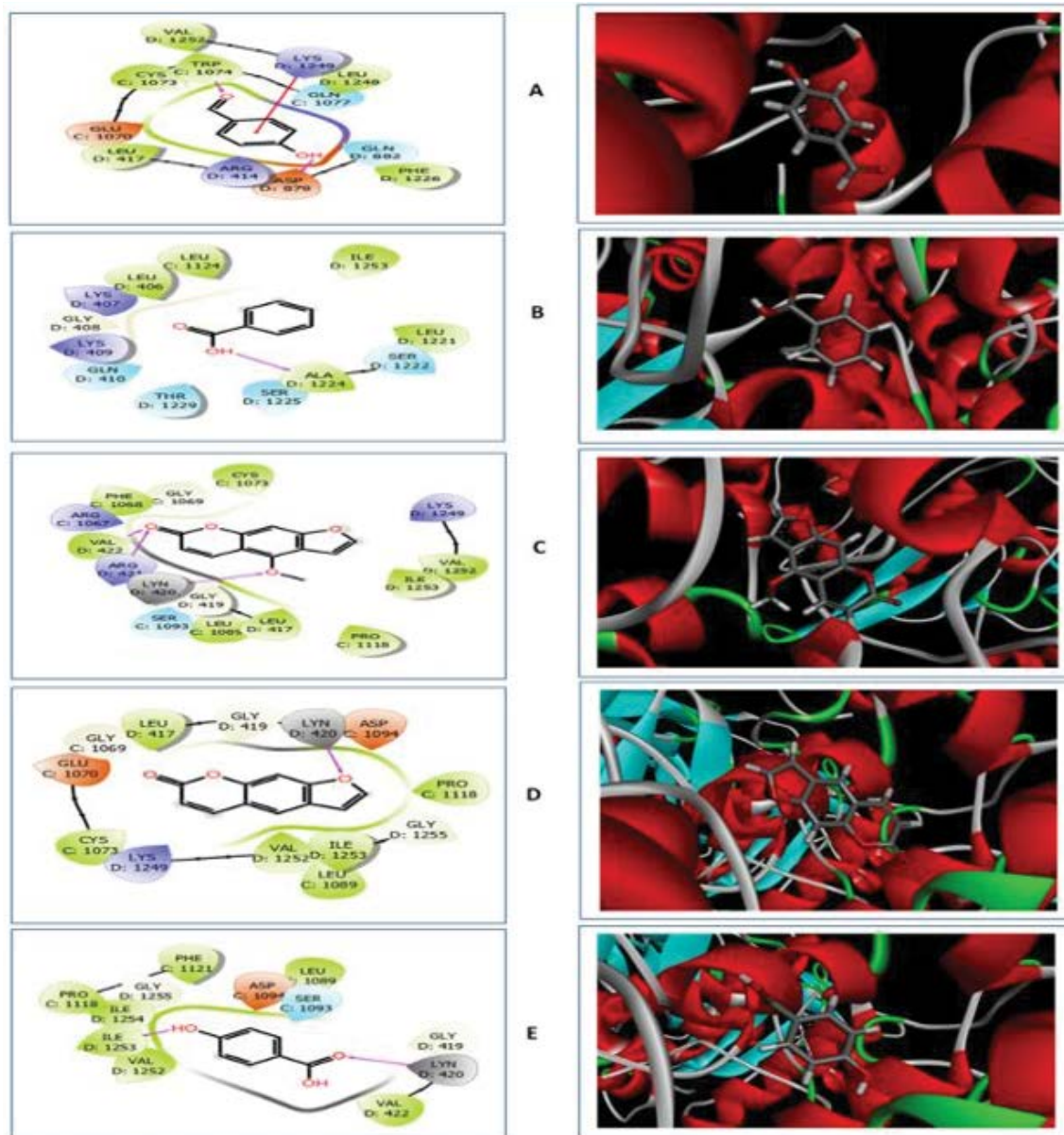


Figure 3: 2D (left) and 3D (right) representations of the best pose interactions between the ligands and the receptor, MTB RNA polymerase. A. interaction between 4-hydroxybenzaldehyde and RNA polymerase, B. interaction between benzoic acid and RNA polymerase, C. interaction between bergapten and RNA polymerase, D. interaction between psoralen and RNA polymerase, E. interaction between p-hydroxybenzoic acid and RNA polymerase. Colored spheres indicate the type of residue in the target: Red-Negatively charged (Asp, Glu), Blue- Polar (Ser, Thr, Gln), Green-Hydrophobic (Ala, Leu, Val, Ile, Trp, Phe, Cys, Pro), Light Purple-Basic (Lys, Arg), Gray- Water molecules, Darker grey-metal atom, Light Yellow- Glycine, Deep Purple-Unspecified molecules and the Grayish circles represent Solvent exposure. Interactions are shown as coloured lines- Solid pink lines with an arrow- H-bond in the target (backbone), Dotted pink lines with an arrow- H-bond between receptor and ligand (side-chain), Solid pink lines without arrow- Metal co-ordination, Green line- Pi-Pi stacking interaction, Green dotted lines- Distances, Partially blue and red-coloured lines- Salt bridges. The grey sphere represents ligands exposed to solvent. The coloured lines show the protein pocket for the ligand according to the nearest atom. Interruptions of the lines indicate the opening of the pocket. In the 3D representations, the proteins are represented in the Solid ribbon model, and the ligands are represented in stick model.

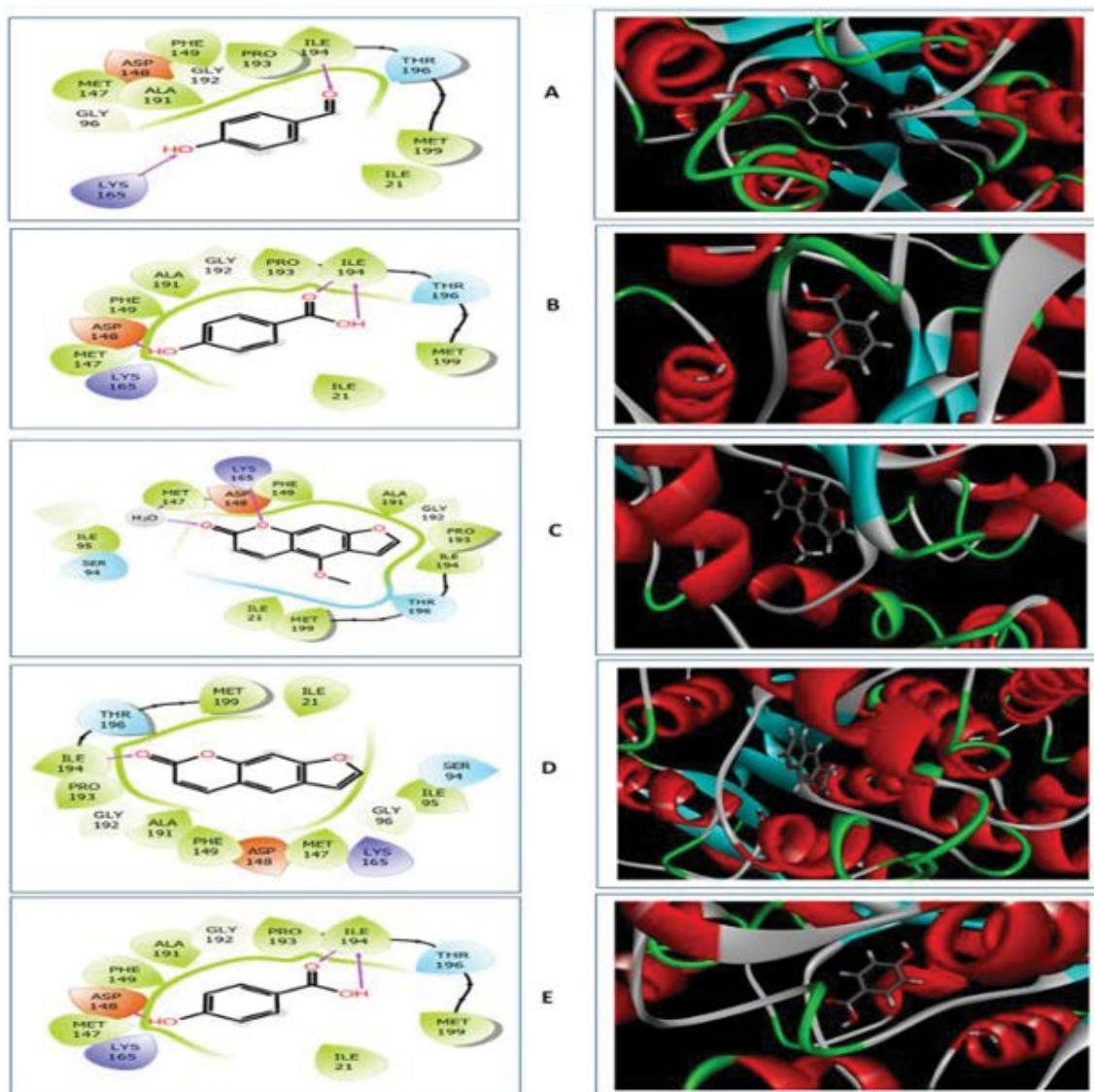


Figure 4: 2D (left) and 3D (right) representations of the best pose interactions between the ligands and the receptor, InhA protein. A. interaction between 4-hydroxybenzaldehyde and InhA protein, B. interaction between benzoic acid and InhA protein, C. interaction between bergapten and InhA protein, D. interaction between psoralen and InhA protein, E. interaction between p-hydroxybenzoic acid and InhA protein. Coloured spheres indicate the type of residue in the target: Red-Negatively charged (Asp), Blue- Polar (Ser, Thr), Green-Hydrophobic (Ala, Ile, Ph, Met, Pro), Light Purple-Basic (Lys), Gray-Water molecules, Darker grey-metal atom, Light Yellow- Glycine, Deep Purple- Unspecified molecules and the Grayish circles represent Solvent exposure. Interactions are shown as coloured lines- Solid pink lines with an arrow- H-bond in the target (backbone), Dotted pink lines with an arrow- H-bond between receptor and ligand (side-chain), Solid pink lines without arrow- Metal co-ordination, Green line- Pi-Pi stacking interaction, Green dotted lines- Distances, Partially blue and red-coloured lines- Salt bridges. A grey sphere represents ligands exposed to solvent. The coloured lines show the protein pocket for the ligand according to the nearest atom. Interruptions of the lines indicate the opening of the pocket. In the 3D representations, the proteins are represented in Solid ribbon model, and the ligands are represented in stick model.

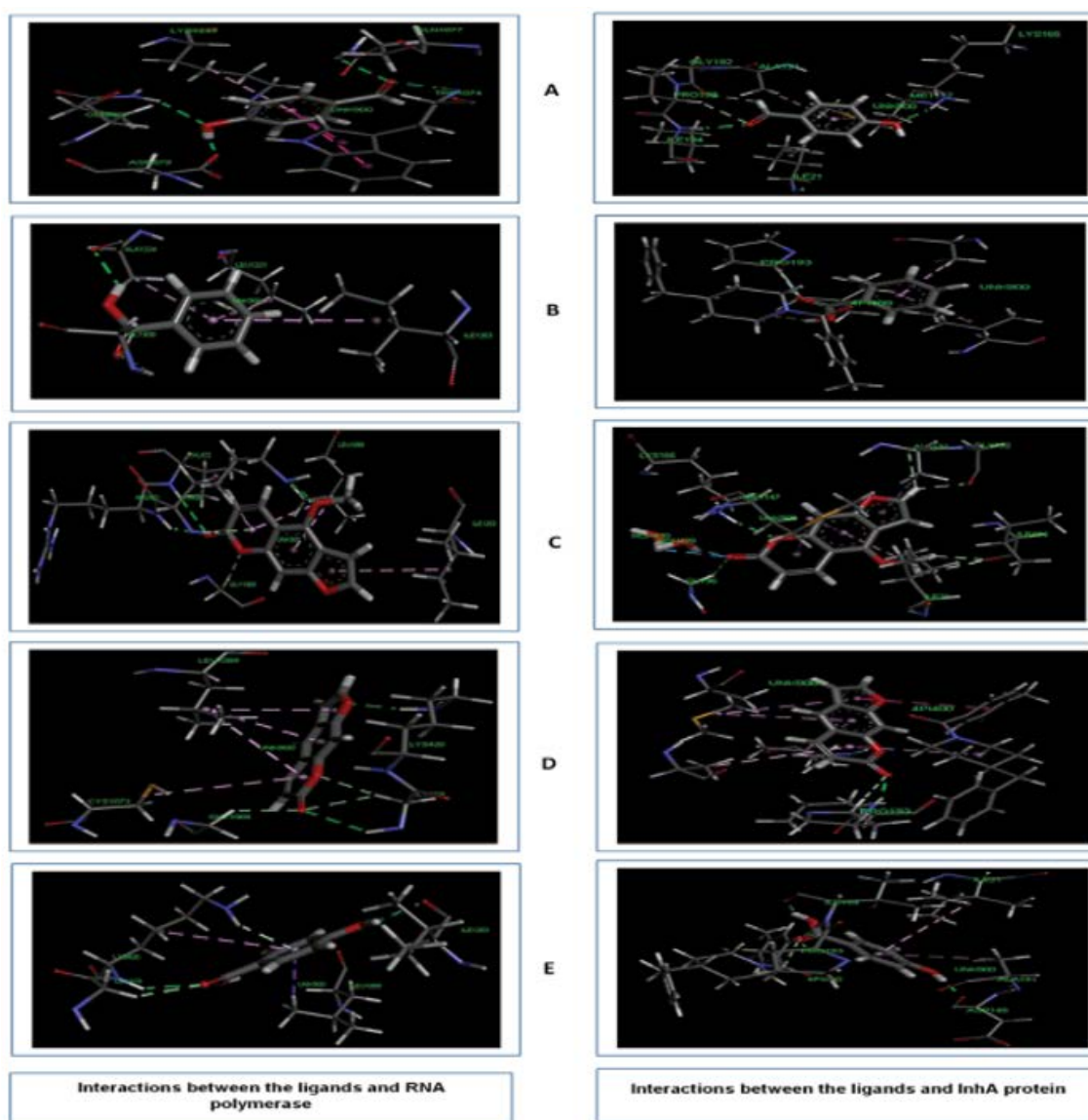


Figure 5: Figure illustrating the different types of bonds and amino acids that participate in the interaction between selected ligands and MTB RNA polymerase (left) as well as InhA protein (right). In this diagram, interacting amino acid residues of the target molecules are labeled. The dotted lines represent the interaction between receptor and ligand, including Purple- Pi-Sigma interaction, Green dotted lines- Conventional bond, Light pink- Alkyl/Pi-Alkyl interactions, Yellow- Pi-Sulfur/Sulphur-X interaction, Orange- Charge-Charge interaction, Red- Donor-Donor interaction, Deep pink- Pi-Pi stacked bond. Here, A. 4-hydroxybenzaldehyde, B. benzoic acid, C. bergapten, D. psoralen, E. p-hydroxybenzoic acid.

bergapten was found to be human hepatotoxic as well as Ames positive. However, bergapten and psoralen showed drug-induced liver injury capability.

P450 Site of Metabolism (SOM) Prediction

The P450 SOM prediction was carried out for the five selected ligand molecules and the SOM prediction was performed for CYPs 1A2, 2A6, 2B6, 2C19, 2C8, 2C9, 2D6, 2E1 and 3A4. 4-hydroxybenzoic acid showed 6 SOMs

for all the CYP450 isoenzymes, and both bergapten and psoralen showed 3 SOMs each, for all the CYP450 isoenzymes. However, benzoic acid showed 6 SOMs for CYP450 1A2 and CYP450 2C8, 4 SOMs for CYP450 2A6 and 5 SOMs for rest of the CYP450 isoenzymes. P-hydroxybenzoic acid showed 5 SOMs for CYP450 2A6, 6 SOMs for CYP450 2E1 and CYP450 3A4 and 7 SOMs for the rest of the CYP450 isoenzymes. The results of P450 SOM are listed in Table 6.

Table 4: Results of the druglikeness property studies of the selected ligand molecules.

Druglikeness properties	4-Hydroxybenzaldehyde	Benzoic acid	Bergapten	Psoralen	p-hydroxybenzoic acid
Lipinski's rule of five	Yes	Yes	Yes	Yes	Yes
Molecular weight (g/mol)	122.12	122.12	216.19	186.16	138.12
Consensus Log P _{ow}	1.17	1.44	2.16	2.12	1.05
Log S	-1.87	-2.2	-2.93	-2.73	-2.07
Num. H-bond acceptors	2	2	4	3	3
Num. H-bond donors	1	1	0	0	2
Molar Refractivity	33.85	33.4	58.75	52.26	35.42
Ghose	No (3 violations)	No (3 violations)	Yes	Yes	No (3 violations)
Veber	Yes	Yes	Yes	Yes	Yes
Egan	Yes	Yes	Yes	Yes	Yes
Muegge	No (1 violation)	No (1 violation)	Yes	No (1 violation)	No (1 violation)
TPSA (Å ²)	37.3	37.3	52.58	43.35	57.53
Druglikeness score	-6.3	-1.4	-3.3	-3.2	-1.5
Drug score	0.17	0.21	0.1	0.27	0.35
Reproductive effective	No	No	Yes (High risk)	No	No
Irritant	Yes (High risk)	Yes (High risk)	No	No	No
Tumorigenic	No	No	Yes (High risk)	No	No
Mutagenic	Yes (High risk)	Yes (High risk)	Yes (High risk)	Yes (High risk)	Yes (High risk)

Table 5: Results of the ADME/T studies of the selected ligand molecules.

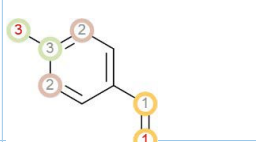
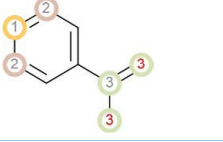
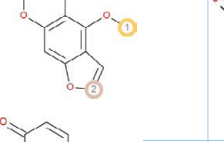
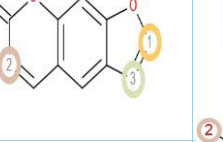
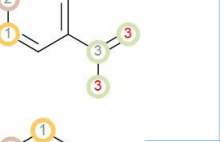
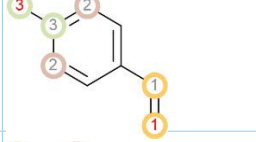
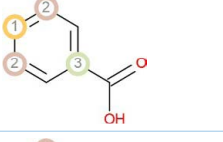
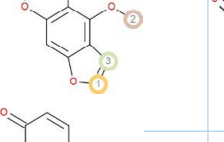
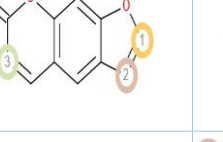
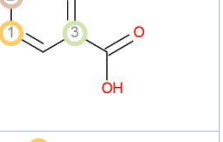
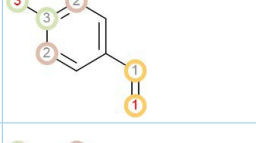
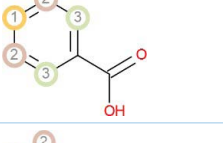
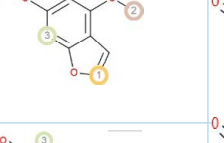
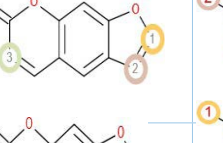
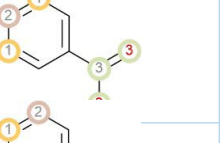
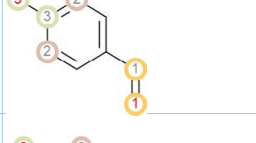
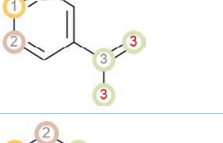
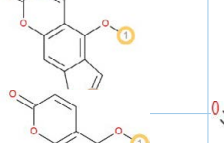
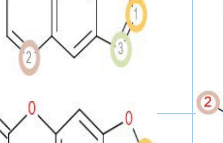
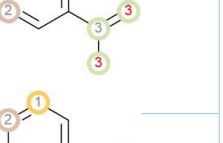
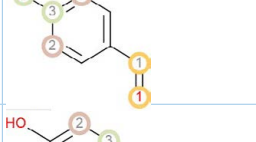
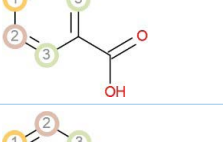
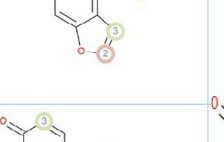
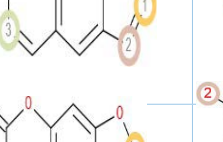
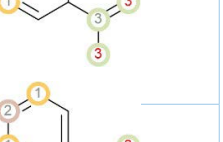
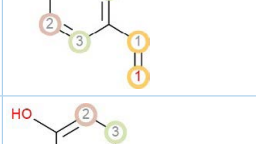
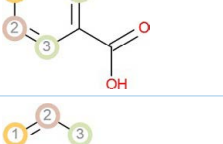
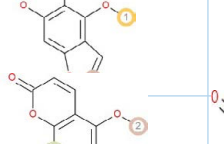
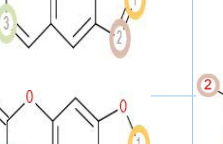
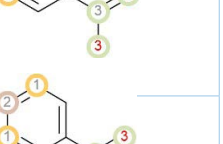
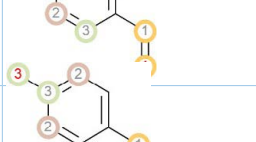
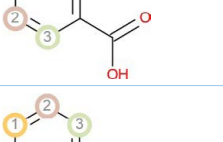
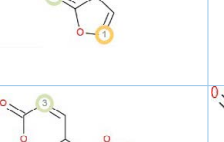
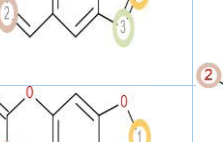
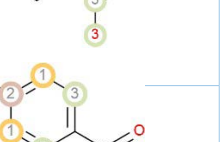
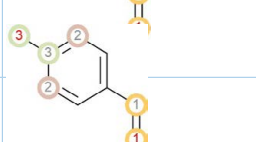
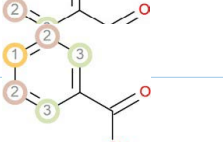
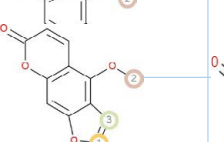
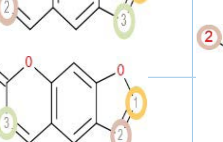
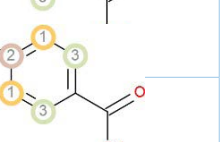
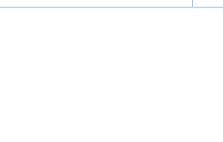
Class	Properties	4-Hydroxybenzaldehyde (with probability)	Benzoic acid (with probability)	Bergapten (with probability)	Psoralen (with probability)	P-hydroxybenzoic acid
Absorption	Caco-2 permeability	Positive (0.965)	Positive (0.953)	Positive (0.819)	Positive (0.863)	Positive (0.923)
	Pgp-inhibitor	Negative (0.987)	Negative (0.989)	Negative (0.878)	Negative (0.934)	Negative (0.986)
	Pgp-substrate	Negative (0.989)	Negative (0.997)	Negative (0.924)	Negative (0.951)	Negative (0.990)
	HIA (Human Intestinal Absorption)	Positive (0.990)	Positive (0.981)	Positive (0.991)	Positive (0.988)	Positive (0.983)
Distribution	PPB (Plasma Protein Binding)	Good, 48.4%	High, 77.7%	High, 79.5%	High, 85.3%	Good, 55.6%
	BBB (Blood-Brain Barrier)	Positive (0.848)	Positive (0.781)	Positive (0.883)	Positive (0.852)	Negative (0.7620)
Metabolism	CYP450 1A2 inhibition	Negative (0.752)	Negative (0.853)	Positive (0.974)	Positive (0.910)	Negative (0.975)
	CYP450 1A2 substrate	-	-	-	-	-
	CYP450 3A4 inhibition	Negative (0.915)	Negative (0.982)	Positive (0.795)	Positive (0.767)	Negative (0.949)
	CYP450 3A4 substrate	Negative (0.795)	Negative (0.879)	Negative (0.607)	Negative (0.753)	Negative (0.826)
	CYP450 2C9 inhibition	Negative (0.985)	Negative (0.986)	Positive (0.825)	Positive (0.534)	Negative (0.969)
	CYP450 2C9 substrate	Negative (0.619)	Negative (0.806)	Negative (1.000)	Negative (1.000)	Negative (0.815)
	CYP450 2C19 inhibition	Negative (0.905)	Negative (0.987)	Positive (0.929)	Positive (0.795)	Negative (0.965)
	CYP450 2C19 substrate	-	-	-	-	-
	CYP450 2D6 inhibition	Negative (0.970)	Negative (0.957)	Positive (0.893)	Positive (0.676)	Negative (0.982)
	CYP450 2D6 substrate	Negative (0.729)	Negative (0.885)	Negative (0.815)	Negative (0.844)	Negative (0.873)
Subcellular localization	Mitochondria	Mitochondria	Mitochondria	Mitochondria	Mitochondria	
Excretion	T _{1/2} (h)	1.7	1.5	0.2	1.423	0.773
Toxicity	hERG (hERG Blockers)	Non-blocker (0.198)	Non-blocker (0.169)	Non-blocker -0.344	Non-blocker -0.298	Non-blocker -0.238
	H-HT (Human Hepatotoxicity)	Negative (0.132)	Negative (0.102)	Positive (0.826)	Negative (0.082)	Negative (0.064)
	Ames (Ames Mutagenicity)	Negative (0.006)	Negative (0.078)	Positive (0.882)	Negative (0.072)	Negative (0.068)
	DILI (Drug Induced Liver Injury)	Negative (0.848)	Negative (0.402)	Positive (0.952)	Positive (0.924)	Negative (0.206)

Pharmacophore Modelling

In the pharmacophore modelling experiment, all the ligands generated pharmacophore hypotheses while inhibiting both MTB RNA polymerase and InhA protein. 4-hydroxybenzaldehyde generated 4-point hypothesis (features: A1, A2, D3, R4) with MTB RNA polymerase and

formed 1 hydrogen bond, 1 pi-cation bond, 3 bad bonds and 1 ugly bond with the binding pocket of the protein. It generated 1-point hypothesis with the InhA protein (feature: A1) and formed 1 pi-pi interaction. Benzoic acid formed 4-point hypothesis (features: A1, A2, D3, R4) while inhibiting the MTB RNA polymerase and formed 1

Table 6: The result of P450 site of metabolism prediction of the selected ligand molecules.

Names of P450 isoenzymes	4- Hydroxybenzaldehyde	Benzoic acid	Bergapten	Psoralen	P-Hydroxybenzoic acid
1A2					
2A6					
2B6					
2C8					
2C9					
2C19					
2D6					
2E1					
3A4					

hydrogen bond and 1 pi-pi interaction within the binding pocket of the receptor. Benzoic acid formed 2-point hypothesis (features: A2, D3) and formed 5 hydrogen bonds and 1 pi-pi interaction within the binding pocket of the receptor protein, InhA protein. Bergapten generated 6-point hypothesis (features: A1, A2, A4, H5, R7, R8) with MTB RNA polymerase and formed 2 bad bonds. However, it generated a 3-point hypothesis (features: A2, H5, R7) with the InhA protein and formed 7 hydrogen bonds, 1 pi-pi interaction and 3 bad bonds within the binding pocket

of the receptor. Psoralen generated 4-point hypothesis (A1, A2, R4, R6) with MTB RNA polymerase, however, it didn't form any bond with the protein. On the other hand, it generated a 3-point hypothesis (features: A1, R4, R6) with InhA protein and formed 1 pi-pi interaction, 1 ugly bond and 3 bad bonds. P-hydroxybenzoic acid generated a 4-point hypothesis (A1, A2, D4, R6) with MTB RNA polymerase and formed 2 hydrogen bonds and 3 bad bonds. Moreover, it generated a 3-point hypothesis (features: A2, D4, D5) with the InhA protein and formed

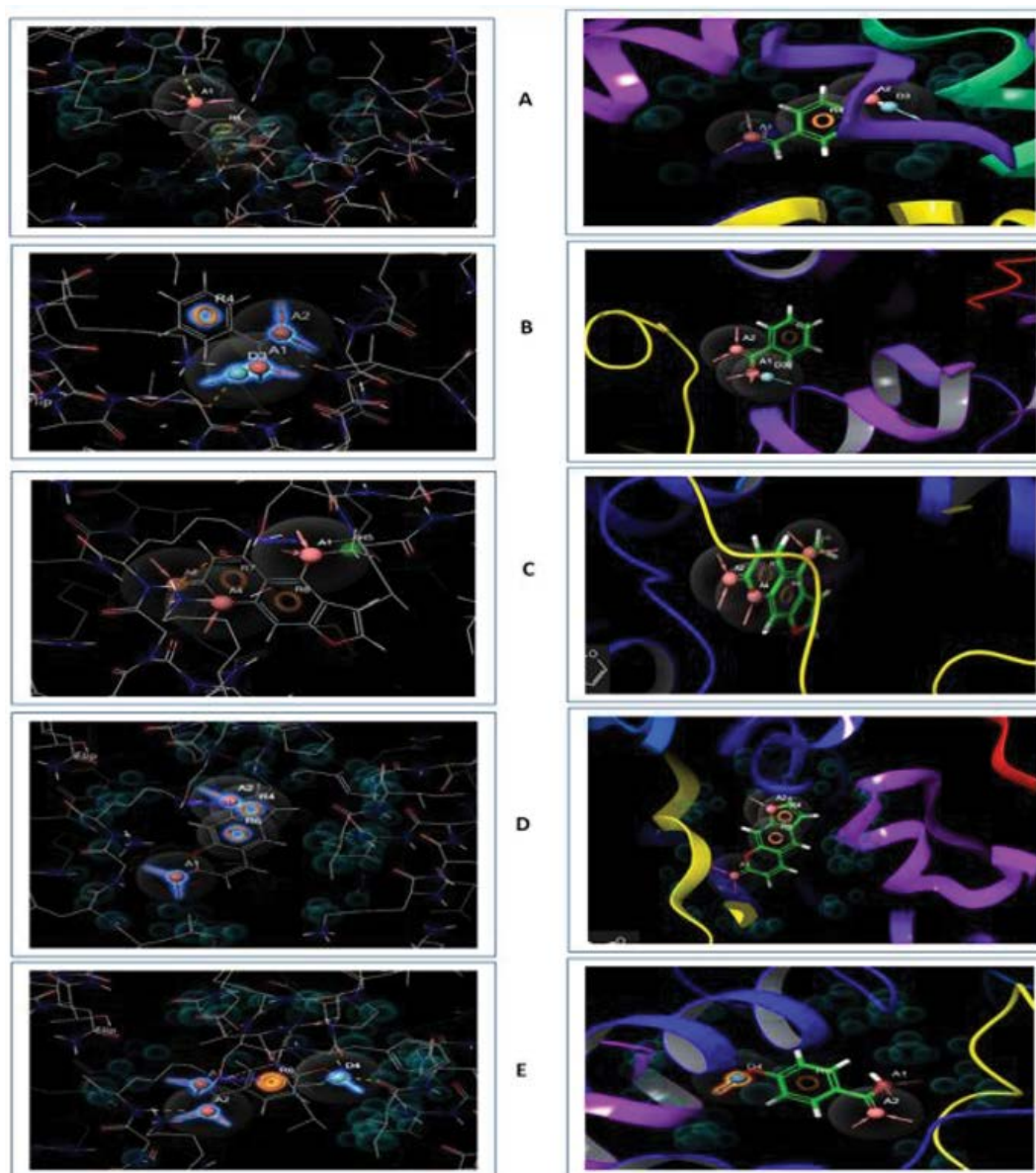


Figure 6: Figure showing the 2D (left) and 3D (right) representations of the pharmacophore hypotheses generated by the ligands while inhibiting the MTB RNA polymerase. Here, A. 4-hydroxybenzaldehyde, B. benzoic acid, C. bergapten, D. psoralen, E. p-hydroxybenzoic acid. The interactions between the ligand and the receptor in the hypothesis were presented by dotted dashed lines, yellow colour-hydrogen bonds and green colour- pi-cation interaction. The bad contacts between the ligands and the pharmacophore are represented. The pharmacophore modelling was carried out by Maestro-Schrödinger Suite 2018-4.

1 pi-pi interaction and 3 bad bonds within the binding pocket of the receptor. However, all the ligands also showed a significant number of good bonds with their receptor proteins (Figures 6 and 7).

Solubility Prediction

The results of the solubility test of all the ligands are listed in Table 7. Bergapten showed the highest QPlogPC16 score of 4.392 and 4-hydroxybenzaldehyde showed the lowest QPlogPC16 score of 2.298. Bergapten also generated the highest QPlogPoct score of 9.129 and the second highest

QPlogPoct score was showed by p-hydroxybenzoic acid. However, both benzoic acid and psoralen showed almost similar QPlogPoct results of 4.474 and 4.881, respectively. Bergapten and p-hydroxybenzoic acid also generated the highest and second-highest QPlogPw scores of 8.804 and 6.296, respectively. However, 4-hydroxybenzaldehyde showed the highest QPlogPo/w value of 0.071 and p-hydroxybenzoic acid generated the highest QPlogS score of 0.948. Benzoic acid showed the highest score of CIQPlogS (-0.284) and bergapten generated the lowest CIQPlogS score of -0.883.

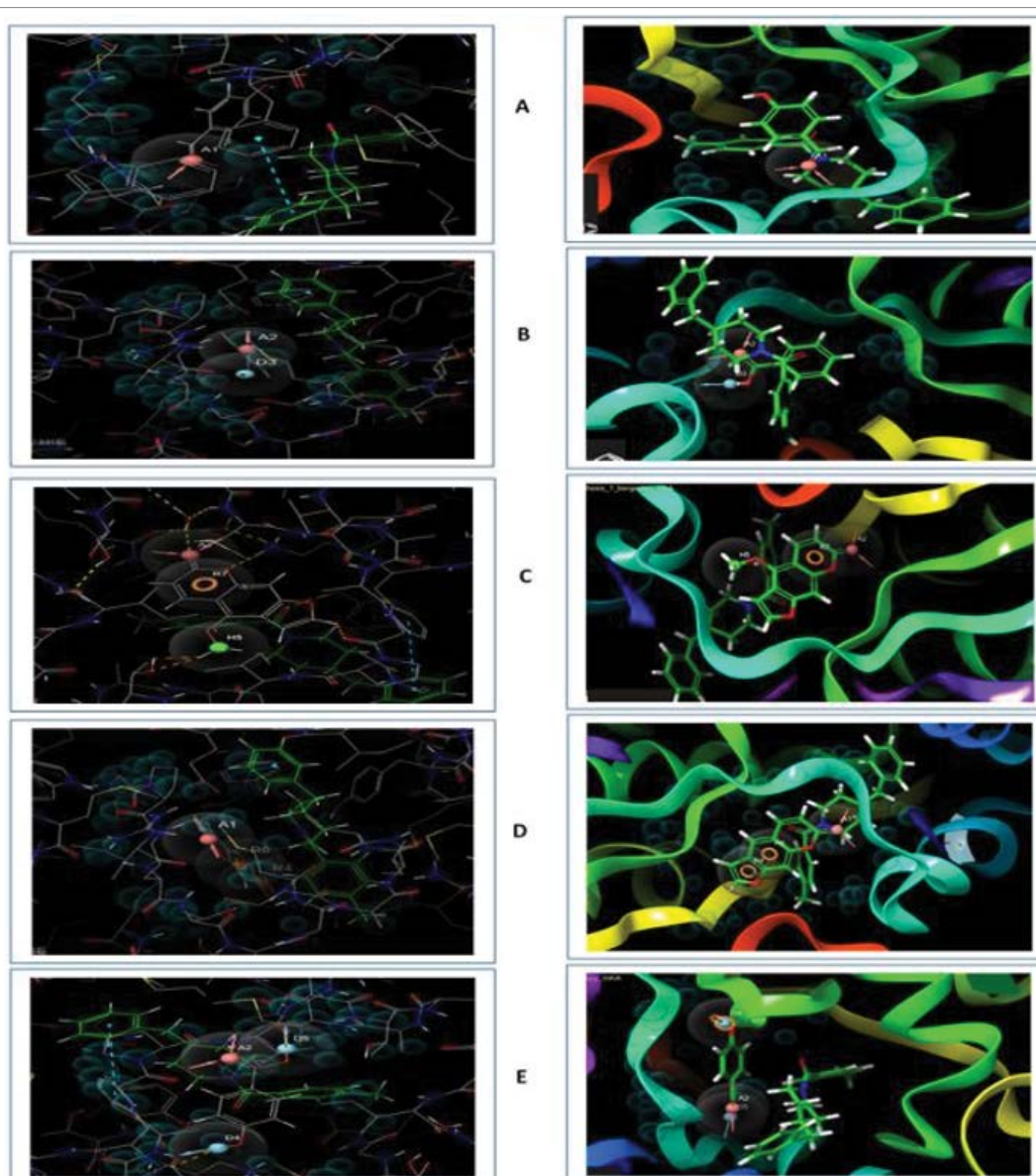


Figure 7: Figure showing the 2D (left) and 3D (right) representations of the pharmacophore hypotheses generated by the ligands while inhibiting the InhA protein. Here, A. 4-hydroxybenzaldehyde, B. benzoic acid, C. bergapten, D. psoralen, E. p-hydroxybenzoic acid. The interactions between the ligand and the receptor were presented by dotted dashed lines, yellow color- hydrogen bonds, and green color- pi-cation interaction. The wrong contacts between the ligands and the pharmacophore are represented. The pharmacophore modeling was carried out by Maestro-Schrödinger Suite 2018-4.

Table 7: List of the solubility tests of the selected ligands. The tests were carried out by QikPrep wizard of Maestro-Schrödinger Suite 2018-4. Here,

Compound Name	QPlogPC16 ^a	QPlogPoct ^b	QPlogPw ^c	QPlogPo/w ^d	QPlogS ^e	CIQPlogS ^f
4-hydroxybenzaldehy de	2.298	3.081	2.406	0.071	0.241	-0.401
Benzoic acid	2.536	4.474	4.803	-0.193	0.097	-0.284
Bergapten	4.392	9.129	8.804	-0.291	-0.714	-0.883
Psoralen	2.989	4.881	4.697	-0.358	0.075	-0.631
P-hydroxybenzoic acid	3.58	6.697	6.296	-0.813	0.948	-0.364

a. Predicted hexadecane/gas partition coefficient (Acceptable range: 4.0 –18.0); b. Predicted octanol/gas partition coefficient (Acceptable range: 8.0–35.0); c. Predicted water/gas partition coefficient (Acceptable range: 4.0–45.0); d. Predicted octanol/water partition coefficient (Acceptable range: –2.0 –6.5); e. Predicted aqueous solubility, S in mol dm⁻³ (Acceptable range: –6.5 – 0.5); f. Conformation-independent predicted aqueous solubility, S in mol dm⁻³(Acceptable range: –6.5 –0.5).

DFT Calculations

Table 8 lists the detailed energy of HOMO, LUMO, Gap, hardness, and softness of the compounds. All the molecules successfully generated the HOMO-LUMO structures. The highest HOMO score or energy was showed by bergapten of -0.112 eV and the lowest was generated by p-hydroxybenzoic acid of -0.198 eV. Psoralen generated quite similar score of p-hydroxybenzoic acid of -0.197 eV. 4-hydroxybenzaldehyde and benzoic acid showed similar scores of -0.174 eV. Psoralen generated the lowest LUMO score of 0.039 eV and p-hydroxybenzoic acid generated the highest LUMO score of 0.100 eV. However, p-hydroxybenzoic acid showed the highest gap score of 0.298 eV and bergapten generated the lowest gap score of 0.164 eV. The molecules showed gap scores of quite similar results. 4-hydroxybenzaldehyde, benzoic acid and psoralen showed quite similar hardness scores of 0.114, 0.115 and 0.118 eV respectively. P-hydroxybenzoic acid gave the highest hardness score of 0.149 eV and bergapten showed the lowest hardness score of 0.082 eV. For this reason, bergapten generated the highest softness score of 12.190 and p-hydroxybenzoic acid generated the lowest softness score of 6.710. Moreover, bergapten generated

the highest dipole moment score of 7.186 debye and benzoic acid generated the lowest dipole moment score of 2.217 debye. The HOMO-LUMO representations of the ligands are shown in Figure 8.

PASS (Prediction of Activity Spectra for Substances) Prediction Study

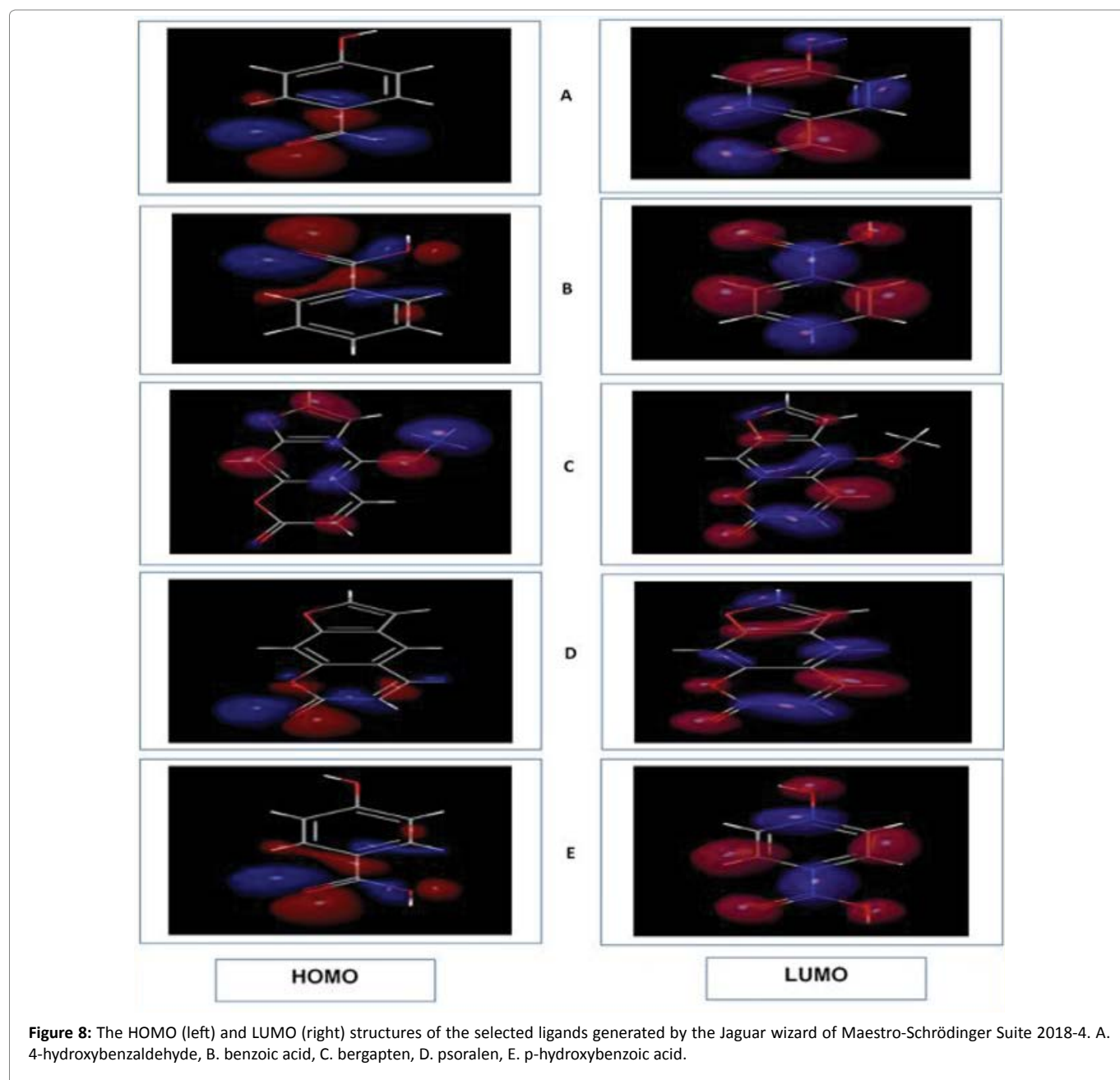
In the PASS prediction study, the predicted LD50 value and toxicity class of 4-hydroxybenzaldehyde were not determined due to the unavailability of data in the server ProTox II. However, bergapten had the predicted LD50 value of 8100 mg/kg and toxicity class of 6. However, the PASS prediction study was conducted for 10 intended biological activities and 5 toxic effects. To carry out the PASS prediction experiment, Pa > 0.7 was kept since this threshold give highly reliable prediction [32]. Both 4-hydroxybenzaldehyde and bergapten showed activities: aldehyde oxidase inhibitor, CYP2A6 substrate, CYP2A substrate, CYP2E1 substrate and CYP1A2 substrate. However, 4-hydroxybenzaldehyde also showed nitrilase inhibitory activity, thioredoxin inhibitory activity and chymosin activity and bergapten also showed activities: HIF1A expression inhibitor and CYP2A11 substrate. The toxic effects showed by 4-hydroxybenzaldehyde were: weakness, vascular toxicity and fatty liver and bergapten showed the toxic effects: hypothermic and carcinogenic group 3. The results of PASS prediction studies are listed in Tables 9 and 10.

DISCUSSIONS

Molecular docking generates a score based on the binding of ligand and receptor. The lower binding affinity is represented by the higher binding energy, whereas

Table 8: The results of the DFT calculations of the selected ligands.

Name of the ligands	HOMO (ineV)	LUMO (ineV)	Gap (ineV)	Hardness (ineV)	Softness (ineV)	Dipole moment (in Debye)
4-hydroxybenzaldehyde	-0.174	0.053	0.227	0.114	8.77	4.839
Benzoic acid	-0.174	0.055	0.229	0.115	8.69	2.217
Bergapten	-0.112	0.052	0.164	0.082	12.19	7.186
Psoralen	-0.197	0.039	0.236	0.118	8.47	5.272
P-hydroxybenzoic acid	-0.198	0.1	0.298	0.149	6.71	2.524



the lower binding energy indicates a higher binding affinity [35,36]. According to the study proofs, the lowest glide energy provides the most appropriate result [37]. The docking of controls, isoniazid and rifampicin was successful with their target receptors. The control produced docking scores of -4.813 Kcal/mol and -6.018 Kcal/mol, respectively as well as glide energies of -25.247 Kcal/mol and -29.728 Kcal/mol, respectively. They generated quite perfect scores in the docking study.

4-hydroxybenzaldehyde exhibited the lowest binding energy of -6.062 Kcal/mol while docked against MTB

RNA polymerase and bergapten provided the lowest score -8.068 Kcal/mol while docked against InhA protein. Nevertheless, 4-hydroxybenzaldehyde generated the glide energy of -21.269 Kcal/mol, which was not exactly a good result since the result was relatively high compared to the other ligands while it was docked with MTB RNA polymerase. On the contrary, bergapten produced the lowest glide energy of -35.218 Kcal/mol, the most suitable score among the ligands when docked against the InhA protein. So, 4-hydroxybenzaldehyde and bergapten should be the best molecules to inhibit their

Table 9: The results of the biological activities PASS prediction study of the two best selected ligands.

SI no	Biological activities	4-Hydroxybenzaldehyde		Bergapten	
		Predicted LD50: NA		Predicted LD50: 8100 mg/kg	
		Toxicity class: NA		Toxicity class: 6	
		Pa	Pi	Pa	Pi
1	Aldehyde oxidase inhibitor	0.951	0.003	0.747	0.013
2	CYP2A6 substrate	0.854	0.004	0.921	0.003
3	CYP2A substrate	0.854	0.004	0.922	0.004
4	CYP2E1 substrate	0.0843	0.004	0.757	0.004
5	CYP1A2 substrate	0.724	0.008	0.75	0.004
6	Nitrilase inhibitor	0.883	0.002	-	-
7	HIF1A expression inhibitor	-	-	0.732	0.017
8	CYP2A11 substrate	-	-	0.923	0.001
9	Thioredoxin inhibitor	0.757	0.005	-	-
10	Chymosin inhibitor	0.76	0.029	-	-

Table 10: The results of the adverse and toxic effects PASS prediction study of the two best selected ligands.

Predicted adverse and toxic effects	4-Hydroxybenzaldehyde		Bergapten	
	Pa	Pi	Pa	Pi
Weakness	0.862	0.011	-	-
Toxic, vascular	0.813	0.015	0.743	0.004
Fatty liver	0.866	0.003	-	-
Hypothermic	-	-	0.73	0.012
Carcinogenic, group 3	0.71	0.021	0.703	0.006

targets. It was further ensured by the MM-GBSA study. In the MM-GBSA study, the ΔG_{Bind} score is taken and the lowest (most negative) ΔG_{Bind} Score is invariably considerable [38-40]. 4-hydroxybenzaldehyde generated a ΔG_{Bind} score of -53.070 Kcal/mol, which was the lowest score among all the ligands while docked against MTB RNA polymerase and bergapten generated a ΔG_{Bind} score of -57.590 Kcal/mol among the ligands while docked against InhA protein. 4-hydroxybenzaldehyde generated 04 hydrogen bonds when docked against MTB RNA polymerase, the second most hydrogen bonds (bergapten was the first ligand with 05 hydrogen bonds). Contrastingly, bergapten generated the highest number of hydrogen bonds (08) when docked against InhA protein. That is why, in the molecular docking experiment, 4-hydroxybenzaldehyde and bergapten were considered the best ligands to inhibit MTB RNA polymerase and InhA protein, respectively (Tables 2 and 3).

Evaluation of drug-likeness properties targets to boost drug discovery and development process. Topological polar surface area (TPSA) and molecular weight influence the drug molecule's permeability through the biological barriers to the pathogen. Higher molecular weight and

TPSA decrease the permeability and conversely. LogP is expressed according to Lipophilicity. It is delineated as the logarithm of the candidate molecule's partition coefficient in the aqueous and the organic phase. The absorption of drug molecules inside the body is influenced by Lipophilicity. Higher LogP denotes lower absorption and inversely [41]. LogS value controls the solubility of a candidate molecule, and the lowest value is favored invariably. Besides, the greater strength of the interaction is indicated by the more significant number of hydrogen bonds and inversely [42-44]. Also, following the Ghose filter, a candidate drug should contain logP value between -0.4 and 5.6, molecular weight between 160 and 480, molar refractivity between 40-130 and the overall number of atoms between 20 and 70, to certify as an efficacious drug [45]. According to the Veber rule, a candidate drug's oral bioavailability relies on two factors: rotatable bonds ≤ 10 and polar surface $\leq 140 \text{ \AA}^2$ [46].

Moreover, as stated by the Egan rule, absorption of a candidate drug molecule counts on two factors: AlogP98 (the logarithm of partition coefficient between n-octanol and water) and the polar surface area (PSA) [47]. Furthermore, The Muegge rule delineates that for a drug

like chemical compound to be considered an effective one, it must undergo a pharmacophore point filter established by some scientists [48]. In line with the drug-likeness property experiment, p-hydroxybenzoic acid should be regarded to be the best molecule because its molecular mass is relatively low (138.12 g/mol). Also, it has a minimal LogP value of 1.05, an elevated drug-likeness score of -1.5 and the supreme drug score of 0.35. Furthermore, it has no allergic properties or tumorigenic effects are almost zero. Notwithstanding, it emerged to be an immensely mutagenic agent that contained the highest TPSA score of 57.53 Å². Psoralen also demonstrated an excellent molecular weight of 186.16 g/mol and reasonably fair LogS value, drug score of 0.27, TPSA score of 43.35 Å² and reproductive effectiveness, tumorigenic effects and irritant properties were absent. Yet, its performance was not so good as p-hydroxybenzoic acid. The performances of other ligand molecules in the drug-likeness studies were quite the same. Even so, all the ligands abide by Lipinski's rule of five. Exclusively, bergapten obeyed the Egan Ghose Muegge and Veber rules of drug-likeness properties. 4-hydroxybenzaldehyde, p-hydroxybenzoic acid and Benzoic acid disobeyed both the Ghose and Muegge rules; also, psoralen infringed the Muegge rule.

The ADME/T-test aims to assess the pharmacodynamic and pharmacological properties of a candidate drug molecule inside the biological system. The blood-brain barrier is distinctly crucial for drugs that predominately target the brain cells. As oral administration is the most widely used route of the drug delivery system; hence, it can be anticipated that this drug's absorption is high in intestinal tissue. The plasma membrane contains P-glycoprotein that expedites the transportation of many drugs. Thus, its inhibition influences the transportation of drug. The *in vitro* study of the drug permeability test uses the Caco-2 cell line and its permeability indicates easy absorption of the drug in the intestine. Drugs that are absorbed orally move across the blood flow and then deposit in the liver. Metabolism of these drugs takes place in the liver by the cytochrome P450 enzyme family. Afterward, the modified inactivated drugs are excreted via urine or bile. Hence, if any enzyme of the cytochrome P450 family enzyme is inhibited, it might alter the biodegradation of the drug molecule [49-51]. A significant pharmacological criterion is the binding of drugs to the membrane-bound protein that affects the pharmacodynamics of the drugs and their circulation and excretion. The competency of a drug confides in the magnitude of its binding with plasma protein. The diffusion of a drug can occur smoothly through the cell

membrane if its binding to the membrane-bound proteins is less effective and vice versa. Drug half-life refers to the time it requires for diminishing the concentration of a drug by 50% inside the body. If a drug's half-life is very high, the drug will remain in the body for a long time. For this reason, the doses of the drug are determined according to its half-life [52-54]. There is a protein found in the heart muscle called HERG, which moderates the heart rhythm. There are various blocking agents, which can block HERG and hampers its activity. This action results not only in cardiac arrhythmia but also in death. The human liver is the principal site of different metabolic reactions. It is intensely sensitive to the adverse and toxic effects of different xenobiotic agents. Human hepatotoxicity (H-HT) is characterized by all forms of injury to the liver, which may eventually cause organ failure and death. A mutagenicity assay called the Ames test is applied for determining the mutagenic chemicals. Mutations are caused by several mutagenic chemicals which can develop cancer. When the administration of any drug causes injury to the liver, it is known as drug induced liver injury (DILI). DILI is one of the causes which may give rise to miscellaneous liver complications [55-76].

CONCLUSION

Five agents known to have potential anti-tubercular properties were used to analyze in the experiment. Considering all the parameters, all the plant-derived anti-tubercular agents had very good inhibitory activities on the MTB. The various tests of *in silico* biology that were used in the experiment, like the molecular docking study, drug-likeness property experiment, ADME/T-test, pharmacological property analysis, solubility and DFT calculations as well as the PASS prediction study had confirmed that 4-hydroxybenzaldehyde and bergapten were best agents among the selected ligands as well as their superiority over the two commercials, widely used drugs, rifampicin and isoniazid. For this reason, these two agents can be used effectively to fight against tuberculosis. 4-hydroxybenzaldehyde can be acquired from a variety of sources from nature, like the plant *Cinnamomum kotoense* and bergapten can be acquired from the plant *Fatoua pilosa*. For this reason, these plants can be used effectively to treat tuberculosis. Moreover, in nature, a lot of other plants can also be found containing these agents. However, more *in vivo* and *in vitro* researches should be carried out to finally confirm their activities. Moreover, more researches should be conducted on the other agents to identify their efficacy against TB since they also gave quite good results in the tests carried out

in the experiment. Hopefully, this study will help the researchers in identifying the potential anti-tubercular phytochemicals.

DECLARATION OF INTEREST

Authors state that they have no conflict of interest among themselves.

REFERENCES

1. Daniel TM. The history of tuberculosis. *Resp Med.* 2006; 100(11):1862-70.
2. Grange JM, Zumla A. The global emergency of tuberculosis: what is the cause? *The journal of the Royal Society for the Promotion of Health.* 2002; 122:78-81.
3. Sepkowitz KA. How contagious is tuberculosis? *Clin Infect Dis.* 1996; 23:954-62.
4. Shah M, Parpio Y, Gul R, Ali A. Educational Needs of Tuberculosis Patients Based On Their Experiences In Karachi, Pakistan. *i-Manager's Journal on Nursing.* 2015; 5:20.
5. Sreeramareddy CT, Panduru KV, Verma SC, Joshi HS, Bates MN. Comparison of pulmonary and extrapulmonary tuberculosis in Nepal-a hospital-based retrospective study. *BMC Infect Dis.* 2008; 8:8.
6. McIlleron H, Wash P, Burger A, Norman J, Folb PI, Smith P. Determinants of rifampin, isoniazid, pyrazinamide, and ethambutol pharmacokinetics in a cohort of tuberculosis patients. *Antimicrob Agents Ch.* 2006; 50(4):1170-77.
7. Ettehad D, Schaaf HS, Seddon JA, Cooke GS, Ford N. Treatment outcomes for children with multidrug-resistant tuberculosis: a systematic review and meta-analysis. *Lancet Infect Dis.* 2012; 12(6):449-56.
8. Rastogi N, David HL. Mode of action of antituberculous drugs and mechanisms of drug resistance in *Mycobacterium tuberculosis*. *Res Microbiol.* 1993; 44(2):133-43.
9. Zhang Y, Wade MM, Scorpio A, Zhang H, Sun Z. Mode of action of pyrazinamide: disruption of *Mycobacterium tuberculosis* membrane transport and energetics by pyrazinoic acid. *J Antimicrob Chemoth.* 2003; 52(5):790-5.
10. Ducasse-Cabanot S, Cohen-Gonsaud M, Marrakchi H, Nguyen M, Zerbib D, Bernadou J, et al. In vitro inhibition of the *Mycobacterium tuberculosis* β -ketoacyl-acyl carrier protein reductase MabA by isoniazid. *Antimicrob Agents Chemother.* 2004; 48(1):242-9.
11. He X, Alian A, de Montellano PR. Inhibition of the *Mycobacterium tuberculosis* enoyl acyl carrier protein reductase InhA by arylamides. *Bioorgan Med Chem.* 2007; 15(21):6649-58.
12. Dong Y, Li J, Qiu X, Yan C, Li X. Expression, purification and crystallization of the (3R)-hydroxyacyl-ACP dehydratase HadAB complex from *Mycobacterium tuberculosis*. *Protein Expr Purif.* 2015; 114:115-20.
13. Molle V, Gulten G, Vilchère C, Veyron-Churlet R, Zanella-Cléon I, Sacchetti JC, et al. Phosphorylation of InhA inhibits mycolic acid biosynthesis and growth of *Mycobacterium tuberculosis*. *Mol Microbiol.* 2010; 78(6):1591-605.
14. Carel C, Nukdee K, Cantaloube S, Bonne M, Diagne CT, Laval F, et al. *Mycobacterium tuberculosis* proteins involved in mycolic acid synthesis and transport localize dynamically to the old growing pole and septum. *PLoS One.* 2014; 9:e97148.
15. Zoete V, Grosdidier A, Michielin O. Docking, virtual high throughput screening and *in silico* fragment-based drug design. *J Cell Mol Med.* 2009; 13(2):238-48.
16. Schneidman-Duhovny D, Nussinov R, Wolfson HJ. Predicting molecular interactions *in silico*: II. Protein-protein and protein-drug docking. *Curr Med Chem.* 2004; 11(1):91-107.
17. Chen FC, Peng CF, Tsai IL, Chen IS. Antitubercular Constituents from the Stem Wood of *Cinnamomum kotoense*. *J Nat Prod.* 2005; 68(9):1318-23.
18. Lim TK. *Hibiscus taiwanensis*. In *Edible Medicinal and Non-Medicinal Plants* 2014; 381-384.
19. Dokorou V, Kovala-Demertzi D, Jasinski JP, Galani A, Demertzi MA. Synthesis, Spectroscopic Studies, and Crystal Structures of Phenylorganotin Derivatives with [Bis (2, 6-dimethylphenyl) amino] benzoic Acid: Novel Antituberculosis Agents. *Helv Chim Acta.* 2004; 87(8):1940-1950.
20. Schrödinger Release 2015-1: Maestro (2015), Schrödinger, LLC, New York, NY.
21. Visualizer, D.S. (2017) Release 4.1. Accelrys Inc., San Diego, CA.
22. Sastry GM, Adzhigirey M, Day T, Annabhimoju R, Sherman W. Protein and ligand preparation: parameters, protocols, and influence on virtual screening enrichments. *J Comput Aid Mol Des.* 2013; 27(3):221-34.
23. LigPrep, Schrödinger, LLC, New York, NY, 2018-4.
24. Cheng F, Li W, Zhou Y, Shen J, Wu Z, Liu G, et al. admetSAR: a comprehensive source and free tool for assessment of chemical ADMET properties.
25. Dong J, Wang NN, Yao ZJ, Zhang L, Cheng Y, Ouyang D, et al. ADMETlab: a platform for systematic ADMET evaluation based on a comprehensively collected ADMET database. *J Cheminformatics.* 2018; 10(1):29.
26. Zaretski J, Bergeron C, Huang TW, Rydberg P, Swamidass SJ, Breneman CM. RS-WebPredictor: a server for predicting CYP-mediated sites of metabolism on drug-like molecules. *Bioinformatics.* 2012; 29(4):497-8.
27. Lee C, Yang W, Parr RG. Development of the Colle-Salvetti correlation-energy formula into a functional of the electron density. *Phys Rev B.* 1988; 37(2):785.
28. Becke AD. Density-functional exchange-energy approximation with correct asymptotic behavior. *Phys Rev A.* 1988; 38(6):3098.
29. Pearson RG. Absolute electronegativity and hardness correlated with molecular orbital theory. *PNAS USA.* 1986; 83(22):8440-1.
30. Parr RG, Yang W. *Density-Functional Theory of Atoms and Molecules*, vol. 16 of International series of monographs on chemistry. 1989. Oxford University Press. New York.
31. Filimonov DA, Lagunin AA, Glorizova TA, Rudik AV, Druzhilovskii DS, Pogodin PV, et al. Prediction of the biological activity spectra of organic compounds using the PASS online web resource. *Chem Heterocycl Com+.* 2014; 50:444-57.
32. Geronikaki A, Poroikov V, Hadjipavlou-Litina D, Filimonov D, Lagunin A, Mgonzo R. Computer aided predicting the biological activity spectra and experimental testing of new thiazole derivatives. *Qsar Comb Sci.* 1999; 18:16-25.
33. Drwal MN, Banerjee P, Dunkel M, Wettig MR, Preissner R. ProTox: a web server for the in-silico prediction of rodent oral toxicity. *Nucleic Acids Res.* 2014; 42: W53-8.
34. Lipinski CA. Lead-and drug-like compounds: the rule-of-five revolution. *Drug Discov Today: Technologies.* 2004; 1(4):337-41.

35. Sarkar B, Islam SS, Ullah MA, Hossain S, Prottoy MN, Araf Y, et al. Computational assessment and pharmacological property breakdown of eight patented and candidate drugs against four intended targets in Alzheimer's disease. *Advances in Bioscience and Biotechnology.* 2019; 10(11):405.
36. Sarkar B, Ullah MA, Araf Y, Das S, Rahman MH, Moin AT. Designing novel epitope-based polyvalent vaccines against herpes simplex virus-1 and 2 exploiting the immunoinformatics approach. *J Biomol Struct Dyn.* 2020; 6:1-21.
37. Raj U, Varadwaj PK. Flavonoids as multi-target inhibitors for proteins associated with Ebola virus: *In silico* discovery using virtual screening and molecular docking studies. *Interdiscip Sci.* 2016; 8(2):132-41.
38. Zhang X, Perez-Sanchez H, C Lightstone F. A comprehensive docking and MM/GBSA rescoring study of ligand recognition upon binding antithrombin. *Curr Top Med Chem.* 2017; 17(14): 1631-39.
39. Ullah MA, Johora FT, Sarkar B, Araf Y, Rahman MH. Curcumin analogs as the inhibitors of TLR4 pathway in inflammation and their drug like potentialities: a computer-based study. *J Recept Signal Transduct Res.* 2020; 40(4):1-5.
40. Sarkar B, Ullah MA, Araf Y. A systematic and reverse vaccinology approach to design novel subunit vaccines against dengue virus type-1 and human Papillomavirus-16. *Informatics in Medicine Unlocked.* 2020; 16:100343.
41. Ullah A, Prottoy NI, Araf Y, Hossain S, Sarkar B, Saha A. Molecular Docking and Pharmacological Property Analysis of Phytochemicals from *Clitoria ternatea* as Potent Inhibitors of Cell Cycle Checkpoint Proteins in the Cyclin/CDK Pathway in Cancer Cells. *Computational Molecular Bioscience.* 2019; 9(03):81.
42. Lipinski CA, Lombardo F, Dominy BW, Feeney PJ. Experimental and computational approaches to estimate solubility and permeability in drug discovery and development settings. *Adv Drug Deliver Rev.* 1997; 23(1-3):3-25.
43. Pollastri MP. Overview on the Rule of Five. *Curr Protoc Pharmacol.* 2010; 49:9-12.
44. Hubbard RE, Kamran Haider M. Hydrogen bonds in proteins: role and strength. *e LS* 2001.
45. Ghose AK, Viswanadhan VN, Wendoloski JJ. A knowledge-based approach in designing combinatorial or medicinal chemistry libraries for drug discovery. 1. A qualitative and quantitative characterization of known drug databases. *J Comb Chem.* 1999; 1(1):55-68.
46. Veber DF, Johnson SR, Cheng HY, Smith BR, Ward KW, Kopple KD. Molecular properties that influence the oral bioavailability of drug candidates. *J Med Chem.* 2002; 45(12):2615-23.
47. Egan WJ, Merz KM, Baldwin JJ. Prediction of drug absorption using multivariate statistics. *Journal Med Chem.* 2000; 43(21):3867-77.
48. Muegge I, Heald SL, Brittelli D. Simple selection criteria for drug-like chemical matter. *J Med Chem.* 2001; 44(12):1841-6.
49. Li AP. Screening for human ADME/Tox drug properties in drug discovery. *Drug Discov Today.* 2001; 6(7):357-366.
50. Guengerich FP. Cytochrome P-450 3A4: regulation and role in drug metabolism. *Annu Rev Pharmacol.* 1999; 39:1-7.
51. Sarkar B, Ullah MA, Islam SS, Rahman MH, Araf Y. Analysis of plant-derived phytochemicals as anti-cancer agents targeting cyclin dependent kinase-2, human topoisomerase IIa and vascular endothelial growth factor receptor-2. *J Recept Signal Transduct Res.* 2020; 12:1-7.
52. Hossain S, Sarkar B, Prottoy MN, Araf Y, Taniya MA, Ullah MA. Thrombolytic activity, drug likeness property and ADME/T analysis of isolated phytochemicals from ginger (*zingiber officinale*) using *in silico* approaches. *Modern Research in Inflammation.* 2019; 8(3):29-43.
53. Swierczewska M, Lee KC, Lee S. What is the future of PEGylated therapies? *Expert Opin Emerg Dr.* 2015; 20(4):531-536.
54. Smalling RW. Molecular biology of plasminogen activators: what are the clinical implications of drug design? *Am J Cardiol.* 1996; 78(12A):2-7.
55. Sanguinetti MC, Jiang C, Curran ME, Keating MT. A mechanistic link between an inherited and an acquired cardiac arrhythmia: HERG encodes the IKr potassium channel. *Cell.* 1995; 81(2):299-307.
56. Aronov AM. Predictive *in silico* modeling for hERG channel blockers. *Drug Discov Today.* 2005; 10(2):149-155.
57. Cheng A, Dixon SL. *In silico* models for the prediction of dose-dependent human hepatotoxicity. *J Comput Aid Mol Des.* 2003; 17:811-823.
58. Mortelmans K, Zeiger E. The Ames Salmonella/microsome mutagenicity assay. *Mutat Res.* 2000; 455(1-2):29-60.
59. Holt MP, Ju C. Mechanisms of drug-induced liver injury. *AAPS J.* 2006; 8:E48-54.
60. Ayers PW, Parr RG, Pearson RG. Elucidating the hard/soft acid/base principle: a perspective based on half-reactions. *J Chem Phys.* 2006; 124(19):194107.
61. Chen JJ, Chou TH, Peng CF, Chen IS, Yang SZ. Antitubercular dihydroagarofuranoid sesquiterpenes from the roots of *Microtropis fokienensis*. *J Nat Prod.* 2007; 70(2):202-5.
62. Chiang CC, Cheng MJ, Peng CF, Huang HY, Chen IS. A novel dimeric coumarin analog and antimycobacterial constituents from *Fatoua pilosa*. *Chem Biodivers.* 2010; 7(7):1728-36.
63. Danielson PB. The cytochrome P450 superfamily: biochemistry, evolution and drug metabolism in humans. *Curr Drug Metab.* 2002; 3(6):561-97.
64. Dixit B. A review on the effects of CMPF binding with Human Serum Albumin. *Bioinformatics Rev.* 2017; 3(9):9-18.
65. Dixon SL, Smondyrev AM, Knoll EH, Rao SN, Shaw DE, Friesner RA. PHASE: a new engine for pharmacophore perception, 3D QSAR model development, and 3D database screening: Methodology and preliminary results. *J Comput Aid Mol Des.* 2006; 20(10-11):647-71.
66. Glue P, Clement RP. Cytochrome P450 enzymes and drug metabolism-basic concepts and methods of assessment. *Cell Mol Neurobiol.* 1999; 19(3):309-23.
67. Hoque MM, Halim MA, Sarwar MG, Khan MW. Palladium-catalyzed cyclization of 2-alkynyl-N-ethanoyl anilines to indoles: synthesis, structural, spectroscopic, and mechanistic study. *J Phys Org Chem.* 2015; 28:732-42.
68. Hussain A, Verma CK. A Combination of Pharmacophore Modeling, Molecular Docking and Virtual Screening Study Reveals 3, 5, 7-Trihydroxy-2-(3, 4, 5-trihydroxyphenyl)-4H-Chromen-4-One as a Potential Anti-Cancer Agent of COT Kinase. *Indian J Pharm Educ.* 2018; 52(4):699-706.
69. Matysiak J. Evaluation of electronic, lipophilic and membrane affinity effects on antiproliferative activity of 5-substituted-2-(2, 4-dihydroxyphenyl)-1, 3, 4-thiadiazoles against various human cancer cells. *Eur J Med Chem.* 2007; 42(7):940-7.
70. Moin AT, Sakib MN, Araf Y, Sarkar B, Ullah MA. Combating COVID-19 Pandemic in Bangladesh: A Memorandum from Developing Country. Preprints. 2020 May 27.

71. Sahin S, Benet LZ. The operational multiple dosing half-life: a key to defining drug accumulation in patients and to designing extended-release dosage forms. *Pharm Res.* 2008; 15:2869-77.
72. Sarkar B, Ullah MA, Prottoy NI. Computational Exploration of Phytochemicals as Potent Inhibitors of Acetylcholinesterase Enzyme in Alzheimer's Disease. *medRxiv.* 2020.
73. Tyzack JD, Mussa HY, Williamson MJ, Kirchmair J, Glen RC. Cytochrome P450 site of metabolism prediction from 2D topological fingerprints using GPU accelerated probabilistic classifiers. *J Cheminformatics.* 2014; 6:29.
74. United Nations. Economic Commission for Europe. Secretariat, 2005. Globally harmonized system of classification and labelling of chemicals (GHS). United Nations Publications.
75. Yuriev E, Ramsland PA. Latest developments in molecular docking: 2010-2011 in review. *J Mol Recognit.* 2013; 26(5):215-39.
76. Zhan CG, Nichols JA, Dixon DA. Ionization potential, electron affinity, electronegativity, hardness, and electron excitation energy: molecular properties from density functional theory orbital energies. *J Phy Chem A.* 2003; 107(20):4184-95.